

---

This is the **accepted version** of the journal article:

De la Peña, Alejandro; Rodríguez-San-Miguel, David; Stylianou, Kyriakos C.; [et al.]. «Direct on-surface patterning of a crystalline laminar covalent organic framework synthesized at room temperature». Chemistry (Weinheim), Vol. 21, issue 30 (July 2015), p. 10666-10670. DOI 10.1002/chem.201501692

---

This version is available at <https://ddd.uab.cat/record/307854>

under the terms of the  **COPYRIGHT** license

# Direct on-Surface Patterning of a Crystalline Laminar Covalent Organic Framework Synthesized at Room Temperature

Alejandro de la Peña Ruigómez,<sup>[a,b]</sup> David Rodríguez-San-Miguel,<sup>[a,c]</sup> Kyriakos C. Stylianou,<sup>[d]</sup> Massimiliano Cavallini,<sup>[e]</sup> Denis Gentili,<sup>[e]</sup> Fabiola Liscio,<sup>[f]</sup> Silvia Milita,<sup>[f]</sup> Otello Maria Roscioni,<sup>[g,h]</sup> Maria Luisa Ruiz-González,<sup>[i]</sup> Carlos Carbonell,<sup>[d]</sup> Daniel Maspocho,<sup>[d,i]</sup> Rubén Mas-Ballesté,<sup>[a]</sup> José Luis Segura,<sup>[b]</sup> and Félix Zamora<sup>\*,[a,c]</sup>

**Communications Abstract:** We report here an efficient, fast and simple synthesis of an imine-based COF at room temperature (hereafter, **RT-COF-1**). **RT-COF-1** shows a layered hexagonal structure exhibiting channels, is robust and is porous to N<sub>2</sub> and CO<sub>2</sub>. The room-temperature synthesis has enabled us to fabricate and position low-cost micro- and submicro-patterns of **RT-COF-1** on several surfaces, including solid SiO<sub>2</sub> substrates and flexible acetate paper, using lithographically controlled wetting and conventional ink-jet printing.

Covalent-Organic Frameworks (COFs) are an emerging class of materials that integrate organic subunits into periodic 2D or 3D porous crystalline structures held together by covalent bonds between elements such as C, B, O, N, and Si.<sup>[1]</sup> They are low-density porous materials (e.g. boronate ester<sup>[1b, 1e, 2]</sup> and imine<sup>[3]</sup>

based COFs) that show a great promise for gas storage and separation.<sup>[1b, 1d, 1f, 1g, 2d, 4]</sup> Recent advances in COFs have been focused on incorporating multifunctional subunits, expanding their scope to numerous practical applications, including catalysis, clean energy, novel ultrasensitive sensors, optoelectronic devices and solar energy collectors.<sup>[1c, 1e, 2f, 3c, 4c, 5]</sup> However, progress in most of these applications is still limited due to the lack of methodologies that allow processing and integrating these materials on supports. In this context, advances have been made in producing thin-films of COFs on several surfaces,<sup>[2a, 6]</sup> but not many in their patterning on surfaces. This is in part because of the current synthetic methods, which generally imply harsh conditions<sup>[1a]</sup> (e.g. high temperatures and pressures) that prevent the use of conventional patterning techniques. To our knowledge, there is only a primary example reported by Dichtel *et al.* who used lithographically patterned single-layer graphene microstructures as chemical affinity templates to selectively grow COF films on them.<sup>[7]</sup> This indirect patterning strategy has allowed preparing microarrays of COFs on rigid SiO<sub>2</sub> surfaces, but not on flexible substrates.

- [a] A.P.R., D.R., Dr. R.M., Dr. F.Z.  
Departamento de Química Inorgánica  
Universidad Autónoma de Madrid  
28049 Madrid (Spain).  
E-mail: felix.zamora@uam.es
- [b] A.P.R., Dr. J.L.S.  
Departamento de Química Orgánica. Fac. de Ciencias Químicas.  
Universidad Complutense de Madrid.  
Avda. Complutense s/n. 28040 Madrid (Spain).
- [c] D.R., Dr. F.Z.  
Instituto Madrileño de Estudios Avanzados en Nanociencia (IMDEA Nanociencia)  
Cantoblanco, 28049 Madrid (Spain).
- [d] Dr. K.C.S., C.C., Prof. D.M.  
ICN2 – Institut Català de Nanociència i Nanotecnologia  
Campus UAB, 08193 Bellaterra (Barcelona), Spain.
- [e] Dr. M.C., Dr. D.G.  
Consiglio Nazionale delle Ricerche. Istituto per lo Studio dei Materiali Nanostrutturati (CNR-ISMN)  
Via Gobetti 101, 40129 Bologna (Italy).
- [f] Dr. F.L., Prof. S.M.  
CNR-IMM, Istituto per la Microelettronica e Microsistemi  
via P. Gobetti 101, I-40129 Bologna (Italy).
- [g] Dr. O.M.R.  
Università di Bologna  
Dipartimento di Chimica Industriale  
"Toso Montanari", Viale Risorgimento 4, 40136, Bologna (Italy).
- [h] Dr. O.M.R.  
School of Chemistry, University of Southampton  
Highfield, Southampton SO17 1BJ (United Kingdom).
- [i] Prof. D.M.  
Institut Catalana de Recerca i Estudis Avançats (ICREA)  
08100 Barcelona (Spain).
- [j] Dr. M.L.R.G.  
Departamento de Química Inorgánica  
Universidad Complutense de Madrid,  
28040 Madrid (Spain)  
Supporting information for this article is given via a link at the end of the document.

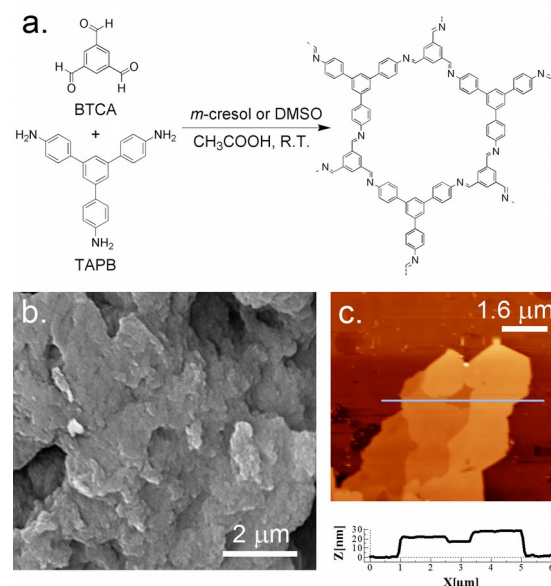


**Figure 1.** a) Schematic illustration of the room-temperature polyimine condensation to form **RT-COF-1**. b) Representative FESEM image of **RT-COF-1**. c) Representative AFM topographic image of isolated flakes of **RT-COF-1** on SiO<sub>2</sub> (top) and the corresponding height profile (bottom).

Lithography-controlled wetting (LCW) and ink-jet printing technologies are powerful techniques that allow the positioning of materials onto surfaces with micron- sub-micron resolution.<sup>[8]</sup>

Here, we report the direct on-surface patterning of COFs on rigid and flexible substrates using both printing technologies. Our approach relies on the rapid and room temperature synthesis of a crystalline laminar imine-based COF (hereafter, **RT-COF-1**).

We show that the Schiff reaction between two trigonal building blocks, 1,3,5-tris(4-aminophenyl)benzene (TAPB) and 1,3,5-benzenetricarbaldehyde (BTCA), rapidly occurs at room temperature and open atmosphere, leading to the formation of **RT-COF-1** (Figure 1a). To date, formation of imine-based polymers has required the use of high temperature, and syntheses at room temperature have been only reported for on-surface synthesized materials.<sup>[3d, 9]</sup> **RT-COF-1** is crystalline showing a laminar hexagonal structure, is stable up to 450 °C, and is porous to both N<sub>2</sub> and CO<sub>2</sub>. Under these specific synthetic conditions, we demonstrate that one can use LCW and ink-jet printing to control the formation of **RT-COF-1** at exact locations of a surface by directly depositing its precursors. We anticipate that this direct patterning strategy allows creating micro- and submicro-structures of **RT-COF-1** either on both rigid and flexible substrates.

**RT-COF-1** was synthesized by adding 1 mL of acetic acid to 10 mL of TAPB and BTCA (1:1 molar ratio; 0.028 M) in either *m*-cresol or DMSO under gentle stirring at room temperature (Figure 1a). After 1 min, a characteristic yellow gel was formed, which was repeatedly washed with methanol and tetrahydrofuran, dried under open atmosphere over 2 days, and further dried at 150 °C under vacuum (50 mbar) overnight to form **RT-COF-1** as a yellow solid (yield: 96 %). The formation of **RT-COF-1** at room temperature was confirmed by solid-state <sup>13</sup>C cross polarization/magic angle spinning nuclear magnetic resonance (CP-MAS NMR) (Figure S3) and FT-IR spectroscopies (Figure S6 and Table S1), and elemental analysis. FT-IR spectrum clearly shows the presence of both imine C=N and C-C=N-C stretching bands at 1617 cm<sup>-1</sup> and 1280 cm<sup>-1</sup>, respectively (Figure S6). The <sup>13</sup>C CP-MAS NMR spectrum is also in agreement with the formation of the imine bonds since it shows: i) a resonance at 157 ppm that corresponds to the carbon atom of the C=N bond; and ii) a resonance at 148 ppm that corresponds to the quaternary carbon atom of the phenyl group of the triamine linked with the nitrogen atom. Finally, its elemental analysis confirmed a molecular formula of C<sub>33</sub>H<sub>26</sub>N<sub>3</sub>O<sub>2.5</sub> for both **RT-COF-1** synthesized in *m*-cresol and DMSO (Section S2). This data is in agreement with the weight loss of 6.6% observed in the thermogravimetric analysis of **RT-COF-1** from 30 to 300 °C, which we attributed to the loss of ca. 2.5 H<sub>2</sub>O molecules (calcd. 7.2 %; Figure S7).

Field-Emission Scanning Electron Microscopy (FESEM) images of the powder demonstrated the formation of uniform aggregates of flakes (Figure 1b). Importantly, we were able to study the shape and dimensions of isolated flakes by depositing a methanolic suspension of **RT-COF-1** on SiO<sub>2</sub> and using Atomic Force Microscopy (AFM). Figure 1c shows characteristic AFM images of isolated flakes, confirming that **RT-COF-1** is based on a laminar structure with sharp edge angles of ca. 60° and 120°, lateral dimensions in the order of several tens of microns, and apparent heights in the range from 4 to 30 nm (see also Figure S8).

Synchrotron radiation Grazing Incidence X-ray Diffraction (GIXRD) performed on samples of **RT-COF-1** directly synthesized on SiO<sub>2</sub> confirmed that they are crystalline. Figures 2a,b depicts the 2D GIXRD patterns of **RT-COF-1** synthesized in *m*-cresol and DMSO, respectively. For both cases, the observation of the same resolved Bragg peaks (*d*-spacing: 15.55, 8.94, 7.71, 5.75, 4.53 and 3.54 Å) in the radially-integrated diffracted intensity profiles provides the signature of the formation of an identical large-scale structure with crystalline organization (Figure 2c). Noticeably, the use of DMSO slightly limits the crystallinity of **RT-COF-1** (supported by the intense halo in the diffraction pattern typical of the amorphous phase). We used the Full Width at High Maximum (FWHM) parameter of the better-resolved Bragg reflections to estimate the size of the crystal domains using the Scherrer equation,<sup>[10]</sup> which were found to be 12 and 9 nm for the **RT-COF-1** synthesized in *m*-cresol and DMSO, respectively. The indexation of Bragg peaks was performed by taking into account the analogies with the powder XRD pattern of a known COF synthesized using trigonal units.<sup>[1b]</sup> The above-mentioned Bragg reflections were indexed as the (001), (110), (200), (210), (220) and (001) diffraction planes, respectively, of a hexagonal unit cell with cell parameters of *a* = *b* = 17.9 ± 0.3 Å and *c* = 3.54 ± 0.03 Å.

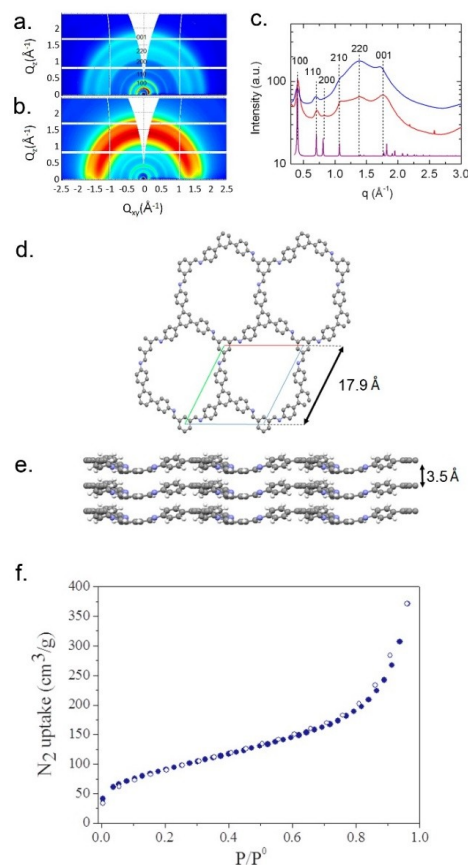


**Figure 2.** a,b) 2D-GIXRD images collected for **RT-COF-1** prepared using *m*-cresol and DMSO as solvents, respectively. c) Radial integration of all the 2D-GIXRD images (line in red for *m*-cresol; in blue for DMSO) and the calculated PXRD for the structure represented in (d). d,e) Schematic views of the crystalline structure of **RT-COF-1** with the unit cell parameters indicated. Carbon, nitrogen and hydrogen are represented as grey, blue and white spheres, respectively. f) N<sub>2</sub> isotherms at 77 K collected on **RT-COF-1**; filled dots: adsorption, empty dots: desorption.



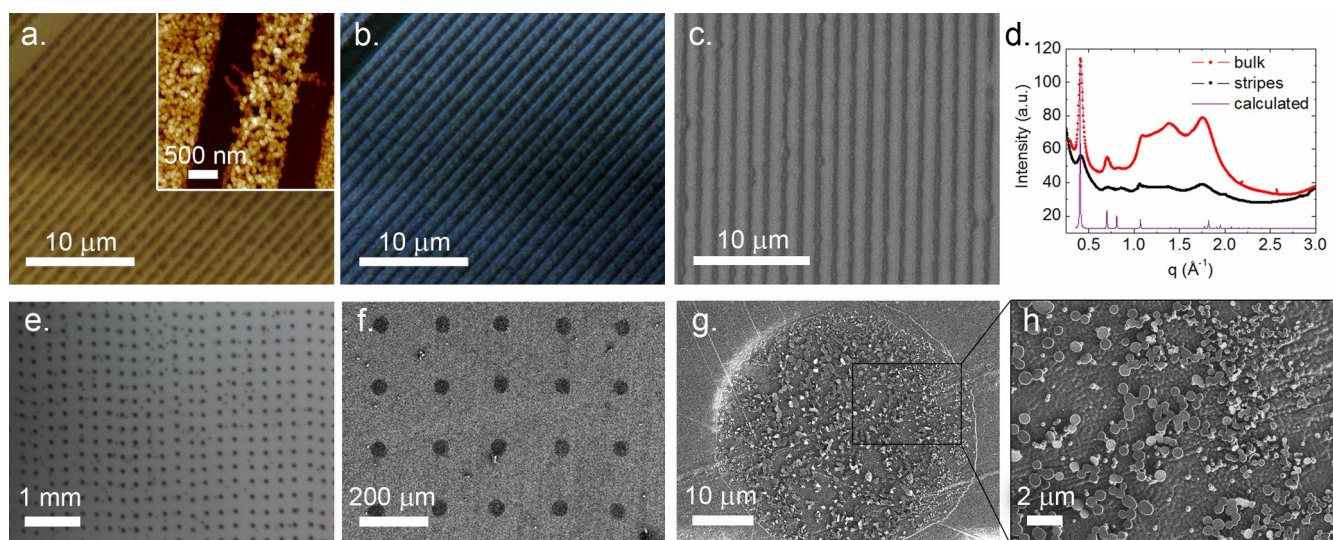


**Figure 3.** a) Bright field optical image of 1  $\mu\text{m}$ -in-width **RT-COF-1** stripes fabricated by LCW. The inset shows a representative AFM image showing the formation of the characteristic **RT-COF-1** flakes. Z scale is 0-50 nm. b) Corresponding POM image. c) Representative FESEM image of 500 nm-in-width **RT-COF-1** stripes fabricated by LCW. d) Radial integration of the 2D-GIXRD image collected for the 1  $\mu\text{m}$ -in-width **RT-COF-1** stripes (black) compared to the one obtained in the synthesis of bulk **RT-COF-1** (red) and to the one derived from the theoretical structure (violet). e) Representative optical image of a 70  $\mu\text{m}$ -in-diameter dot array of **RT-COF-1** on  $\text{SiO}_2$  generated by inkjet printer. f) Representative FESEM image of a 40  $\mu\text{m}$ -in-diameter dot array of **RT-COF-1** on flexible acetate paper generated by ink-jet printer. g,h) Zoomed FESEM images of one of these dots, showing again the formation of the characteristic **RT-COF-1** flakes.

To gain more insights on the crystal structure of **RT-COF-1**, we performed plane-wave density functional theory (DFT) calculations constraining the cell parameters determined from GIXRD data. For detailed information on these calculations, see Section S8. We found that a structure with a trigonal P3 space group is the most energetically stable. This structure is likely to be the correct one due to the similarity found between the simulated powder XRD derived from the structure and the experimental one obtained in grazing incidence and specular geometries (Figure 2c). The structure shows that a laminar framework in which the imine-based sheets are stacked in an AA fashion (separation between sheets: 3.5 Å; Figure 2e), resulting in the formation of 1D hexagonal-shaped pores with dimensions of 11.9 Å  $\times$  11.9 Å (including van der Waals radii) along the *c*-axis (Figure 2d). The solvent accessible volume of **RT-COF-1** determined using PLATON<sup>[11]</sup> is 50 % per unit cell.

Transmission electron microscopy analysis of **RT-COF-1** confirms the presence of nanodomains exhibiting periodicities of 1.2 nm (Figure S13). This distance fits well to the pore dimensions of **RT-COF-1**. A careful analysis allows infer the hexagonal distribution of pores (Section S9). The absence of a long range ordered hexagonal distribution is in agreement to the GIXRD apart from the degradation induced under the electron beam.

Thermal treatment of **RT-COF-1** at 150 °C and 10<sup>-3</sup> bar overnight produced the activation of the material (Figure S14). Nitrogen isotherms were performed to confirm the permanent porosity of the activated **RT-COF-1** at 77 K. From the N<sub>2</sub> isotherm, the BET surface area was found to be 329 m<sup>2</sup>/g in the range of  $p/p^0 = 0.05$ -0.3 (Figure 2f) which is close to other values recently reported for similar imine-linked COFs.<sup>[3c, 12]</sup> The fitting of the N<sub>2</sub> adsorption data to the Dubinin-Radushkevich equation provides a pore volume of 0.224 cm<sup>3</sup>/g (Figure S15).

**RT-COF-1** is also porous to CO<sub>2</sub> at 195, 273 and 298 K, with a BET surface area calculated from the CO<sub>2</sub> adsorption ( $p/p^0 = 0.05$ -0.3) of 369 m<sup>2</sup>/g (Figure S16). The strength of interactions between **RT-COF-1** and CO<sub>2</sub> was evaluated using the Clausius-Clapeyron equation.<sup>[13]</sup> It was found that the isosteric heat of adsorption is 16.4 kJ/mol at zero coverage, whereas it is

between 15.1 to 18.1 kJ/mol at high loadings (Figure S17). This constant value suggests that the interactions between CO<sub>2</sub> and **RT-COF-1** are strong either at zero coverage or high loadings due to the presence of Lewis basic imine groups.

It is worth mentioning that besides insoluble COFs, soluble porous cage compounds have been demonstrated to be processed on surfaces for several purpose.<sup>[14]</sup> Here, the soft reaction conditions required for the preparation of **RT-COF-1** allowed to overcome the typical limitations of COF-based materials to be deposited on surfaces in a controlled manner. Our approach relied on confining the room temperature synthesis of **RT-COF-1** into small volumes containing the **RT-COF-1** precursors, which were previously patterned on surfaces. We first fabricated **RT-COF-1** stripes on  $\text{SiO}_2$  substrates using lithographically controlled wetting (LCW). LCW is a simple, fast and sustainable wet patterning process that exploits the self-organization of soluble materials under the protrusion of a soft stamp (Section S11).<sup>[8a-c]</sup> **RT-COF-1** stripes were fabricated by patterning an *m*-cresol solution of TAPB and BTCA into 1  $\mu\text{m}$ -in-width microchannels of a PDM stamp (Scheme S2). Then, acetic acid was poured at the beginning of the microchannels, confining the **RT-COF-1** synthesis into these channels. Figure 3a,b shows the resulting 1  $\mu\text{m}$ -in-width **RT-COF-1** stripes after removing the stamp. We could also reduce the size of the stripes by using a PDM stamp with thinner channels (width = 500 nm), resulting in thinner 500 nm-in-width **RT-COF-1** stripes (Figure 3c).

GIXRD, polarized optical microscopy (POM) and AFM were used to characterize the patterned stripes (Figures 3a-d). Importantly, GIXRD performed on the 1  $\mu\text{m}$ -in-width **RT-COF-1** stripes showed a powder XRD spectrum that coincides with those derived from the structure and from the bulk synthesis (Figure 3d). This evidence confirms that **RT-COF-1** maintained its crystal structure once synthesized and structured on surfaces. The crystallinity of the stripes was also corroborated by POM, which images show a slight birefringence (Figure 3b). Here, the stripes appeared homogeneously colored in blue, indicating that their mean thickness is almost constant over the entire stripe and therefore, that the confined synthesis by LCW

has induced a coherent order along the direction of the stripes. Finally, a detailed investigation of the stripes by AFM showed that they are formed by the characteristic flakes of **RT-COF-1**, which size range from 25 to 100 nm (inset of Figure 3a). It is important to note here is that the fabricated stripes showed to be stable after a few months from preparation as well as after their treatment with water and alcohol solutions.

To expand the diversity of surfaces as well as to prove the scalability of the patterning, we also explored ink-jet printing. Inject printing is a scale-up and inexpensive patterning technology that enable the organization of materials in a variety of surfaces, including rigid and flexible substrates.<sup>[8d]</sup> Accordingly, we fabricated large dot arrays of **RT-COF-1** on both rigid SiO<sub>2</sub> surfaces (Figure 3e) and flexible acetate paper (Figures 3f-h) by simply depositing an ink consisting of a stoichiometric DMSO solution of TAPB and BTCA using a commercial Dimatrix Fuji ink-jet printer. In both type of surfaces, all printed patterns show significant uniformity and resolution (dot size controlled from 50 to 70  $\mu\text{m}$ ), confirming the reliability and efficiency of the printing over extensions of 1 cm<sup>2</sup>. The printed structures on SiO<sub>2</sub> and acetate paper were characterized by optical microscopy, FESEM and AFM (Figure 3e-h and Figures S19-20), showing in all cases the characteristic formation of flakes of **RT-COF-1**.

In conclusion, we have reported the synthesis of an extended imine-based COF using a simple and one-pot reaction at room temperature. Under these conditions, **RT-COF-1** is crystalline with hexagonal structure, possesses pronounced thermal stability and is permanently porous to N<sub>2</sub> and CO<sub>2</sub>. We have demonstrated that the room temperature synthesis of **RT-COF-1** can be miniaturized on surfaces by using a soft-lithography technique and ink-jet printing. Both techniques have allowed the fabrication of micro/submicrometer patterns of **RT-COF-1** on solid and flexible supports that enable future applications. The preliminary results using ink-jet printing are very promising for automation and enables patterning with high resolution covering large areas in minutes, therefore being attractive for manufacturing. Ongoing studies focus on the expansion of the family of RT-COFs and study their tailored properties when are already integrated on surfaces.

## Acknowledgements

We thank the MINECO (Spain) for financial support through projects MAT2013-46753-C2-1-P, MAT2012-30994 and CTQ2010-14982). AP acknowledges UCM for a predoctoral fellowship. Support from the EPSRC (UK) National Service for Computational Chemistry Software is acknowledged.

**Keywords:** covalent organic frameworks • porous crystalline materials • processability • soft-lithography • ink-jet printing

- [1] a) S. Y. Ding, W. Wang, *Chem. Soc. Rev.* **2013**, 42, 548-568; b) A. P. Cote, A. I. Benin, N. W. Ockwig, M. O'Keeffe, A. J. Matzger, O. M. Yaghi, *Science* **2005**, 310, 1166-1170; c) S. Wan, J. Guo, J. Kim, H. Ihee, D. L. Jiang, *Angew. Chem Int. Ed.* **2008**, 47, 8826-8830; d) R. W. Tilford, W. R. Gemmill, H. C. zur Loye, J. J. Lavigne, *Chem. Mater.* **2006**, 18, 5296-5301; e) E. L. Spitler, W. R. Dichtel, *Nat. Chem.* **2010**, 2, 672-677; f) R. W. Tilford, S. J. Mugavero, P. J. Pellechia, J. J. Lavigne, *Adv. Mater.* **2008**, 20, 2741-2744; g) H. M. El-Kaderi, J. R. Hunt, J. L. Mendoza-Cortes, A. P. Cote, R. E. Taylor, M. O'Keeffe, O. M. Yaghi, *Science* **2007**, 316, 268-272; h) J. X. Jiang, A. I. Cooper, *Top. Curr. Chem.* **2010**, 293, 1-33.
- [2] a) J. W. Colson, A. R. Woll, A. Mukherjee, M. P. Levendorf, E. L. Spitler, V. B. Shields, M. G. Spencer, J. Park, W. R. Dichtel, *Science* **2011**, 332, 228-231; b) J. F. Dienstmaier, A. M. Gigler, A. J. Goetz, P. Knochel, T. Bein, A. Lyapin, S. Reichmaier, W. M. Heckl, M. Lackinger, *ACS Nano* **2011**, 5, 9737-9745; c) Z. Kahveci, T. Islamoglu, G. A. Shar, R. Ding, H. M. El-Kaderi, *CrystEngComm* **2013**, 15, 1524-1527; d) A. P. Cote, H. M. El-Kaderi, H. Furukawa, J. R. Hunt, O. M. Yaghi, *J. Am. Chem. Soc.* **2007**, 129, 12914-12915; e) A. Nagai, Z. Q. Guo, X. Feng, S. B. Jin, X. Chen, X. S. Ding, D. L. Jiang, *Nat Commun.* **2011**, 2, 536; f) X. A. Feng, L. Chen, Y. P. Dong, D. L. Jiang, *Chem. Commun.* **2011**, 47, 1979-1981.
- [3] a) S. L. Cai, Y. B. Zhang, A. B. Pun, B. He, J. H. Yang, F. M. Toma, I. D. Sharp, O. M. Yaghi, J. Fan, S. R. Zheng, W. G. Zhang, Y. Liu, *Chem. Sci.* **2014**, 5, 4693-4700; b) S. B. Jin, T. Sakurai, T. Kowalczyk, S. Dalapati, F. Xu, H. Wei, X. Chen, J. Gao, S. Seki, S. Irle, D. L. Jiang, *Chem. Eur. J.* **2014**, 20, 14608-14613; c) S. Y. Ding, J. Gao, Q. Wang, Y. Zhang, W. G. Song, C. Y. Su, W. Wang, *J. Am. Chem. Soc.* **2011**, 133, 19816-19822; d) X. H. Liu, C. Z. Guan, S. Y. Ding, W. Wang, H. J. Yan, D. Wang, L. J. Wan, *J. Am. Chem. Soc.* **2013**, 135, 10470-10474; e) M. G. Rabbani, A. K. Sekizkardes, Z. Kahveci, T. E. Reich, R. S. Ding, H. M. El-Kaderi, *Chem. Eur. J.* **2013**, 19, 3324-3328.
- [4] a) J. X. Jiang, F. Su, A. Trewin, C. D. Wood, H. Niu, J. T. A. Jones, Y. Z. Khimyak, A. I. Cooper, *J. Am. Chem. Soc.* **2008**, 130, 7710-7720; b) F. J. Uribe-Romo, J. R. Hunt, H. Furukawa, C. Klock, M. O'Keeffe, O. M. Yaghi, *J. Am. Chem. Soc.* **2009**, 131, 4570-4572; c) H. Furukawa, O. M. Yaghi, *J. Am. Chem. Soc.* **2009**, 131, 8875-8883; d) C. J. Doonan, D. J. Tranchemontagne, T. G. Glover, J. R. Hunt, O. M. Yaghi, *Nat. Chem.* **2010**, 2, 235-238.
- [5] a) P. Kuhn, M. Antonietti, A. Thomas, *Angew. Chem Int. Ed.* **2008**, 47, 3450-3453; b) E. L. Spitler, M. R. Giovino, S. L. White, W. R. Dichtel, *Chem. Sci.* **2011**, 2, 1588-1593; c) X. S. Ding, J. Guo, X. A. Feng, Y. Honsho, J. D. Guo, S. Seki, P. Maitarad, A. Saeki, S. Nagase, D. L. Jiang, *Angew. Chem Int. Ed.* **2011**, 50, 1289-1293.
- [6] a) D. D. Medina, V. Werner, F. Auras, R. Tautz, M. Dogru, J. Schuster, S. Linke, M. Dobliger, J. Feldmann, P. Knochel, T. Bein, *ACS Nano* **2014**, 8, 4042-4052; b) E. L. Spitler, B. T. Koo, J. L. Novotny, J. W. Colson, F. J. Uribe-Romo, G. D. Gutierrez, P. Clancy, W. R. Dichtel, *J. Am. Chem. Soc.* **2011**, 133, 19416-19421; c) E. L. Spitler, J. W. Colson, F. J. Uribe-Romo, A. R. Woll, M. R. Giovino, A. Saldivar, W. R. Dichtel, *Angew. Chem Int. Ed.* **2012**, 51, 2623-2627.
- [7] J. W. Colson, J. A. Mann, C. R. DeBlase, W. R. Dichtel, *J. Polym. Sci. A, Polym. Chem.* **2015**, 53, 378-384.
- [8] a) M. Cavallini, D. Gentili, P. Greco, F. Valle, F. Biscarini, *Nat. Prot.* **2012**, 7, 1569-1764; b) M. Cavallini, C. Albonetti, F. Biscarini, *Adv. Mater.* **2009**, 21, 1043-1053; c) M. Cavallini, F. Biscarini, *Nano Lett.* **2003**, 3, 1269-1271; d) V. Subramanian (Eds.: J. P. Korvink, P. J. Smith, D.-Y. Shin), Wiley-VCH, Weinheim, Germany, **2012**, pp. 313-329.
- [9] a) M. G. Schwab, B. Fassbender, H. W. Spiess, A. Thomas, X. L. Feng, K. Mullen, *J. Am. Chem. Soc.* **2009**, 131, 7216-7218; b) X. D. Zhuang, F. Zhang, D. Q. Wu, X. L. Feng, *Adv. Mater.* **2014**, 26, 3081-3086; c) L. R. Xu, X. Zhou, Y. X. Yu, W. Q. Tian, J. Ma, S. B. Lei, *ACS Nano* **2013**, 7, 8066-8073.
- [10] B. E. Warren, *X-Ray Diffraction*, Addison-Wesley, **1969**.
- [11] A. L. Spek, *Acta Crystall. D* **2009**, 65, 148-155.
- [12] a) S. Kandambeth, A. Mallick, B. Lukose, M. V. Mane, T. Heine, R. Banerjee, *J. Am. Chem. Soc.* **2012**, 134, 19524-19527; b) P. Pachfule, M. K. Panda, S. Kandambeth, S. M. Shivaprasad, D. D. Diaz, R. Banerjee, *J. Mater. Chem. A* **2014**, 2, 7944-7952; c) Y. H. Jin, Y. L. Zhu, W. Zhang, *CrystEngComm* **2013**, 15, 1484-1499; d) P. Pandey, A. P. Katsoulidis, I. Eryazici, Y. Y. Wu, M. G. Kanatzidis, S. T. Nguyen, *Chem. Mater.* **2010**, 22, 4974-4979.
- [13] K. Sumida, D. L. Rogow, J. A. Mason, T. M. McDonald, E. D. Bloch, Z. R. Herm, T. H. Bae, J. R. Long, *Chem. Rev.* **2012**, 112, 724-781.
- [14] a) M. J. Boidys, T. Hasell, N. Severin, K. E. Jelfs, J. P. Rabe, A. I. Cooper, *Chem. Commun.* **2012**, 48, 11948-11950; b) M. Brutschy, M. W. Schneider, M. Mastalerz, S. R. Waldvogel, *Adv. Mater.* **2012**, 24, 6049-6051; c) M. Brutschy, M. W. Schneider, M. Mastalerz, S. R. Waldvogel, *Chem. Commun.* **2013**, 49, 8398-8400.

## Entry for the Table of Contents

---

*A. Peña Ruigómez, D. Rodríguez-San-Miguel, K. C. Stylianou, M. Cavallini, D. Gentili, F. Liscio, S. Milita, O. María Roscioni, C. Carbonell, D. Maspoch, R. Mas-Ballesté, J. L. Segura, F. Zamora\**

**Text for Table of Contents:** An efficient, fast and simple synthesis of an imine-based porous COF at room temperature is reported. The room-temperature synthesis enables fabricating micro- and submicro-patterns of this COF on a variety of surfaces by ink-jet printing and wet lithographically techniques.

**Surface Patterning of a Crystalline Laminar Covalent Organic Framework Synthesized at Room Temperature**

